

MOORING SYSTEM STIFFNESS: A GENERAL ANALYTICAL FORMULATION WITH AN APPLICATION TO FLOATING OFFSHORE WIND TURBINES

Celso P. Pesce

(ceppesce@usp.br)

Giovanni A. Amaral

(giovanni.amaral@usp.br)

Guilherme R. Franzini

(gfranzini@usp.br)

Escola Politécnica – University of São Paulo
LMO - Offshore Mechanics Laboratory
São Paulo, SP, Brazil

ABSTRACT

Using classic approaches of analytical mechanics, this paper addresses the general problem and provides an analytic and explicit formulation for the stiffness matrix of a generic mooring system layout. This is done around a generic offset position and heading of the floating unit, given the curves of tension vs displacement for each mooring line, for a frictionless seabed. The international benchmark of the Offshore Code Comparison Collaboration Continuation – OC4 is taken as a case study. The use of the analytical formulation is exemplified by systematically varying the mean offset position and heading of the platform, as well as the pre-tensioning of the mooring system.

Keywords: mooring system, stiffness, analytic formulation, floating wind turbine, OC4.

INTRODUCTION

Mooring system design is an essential task in Floating Offshore Wind Turbine (FOWT) projects. A good mooring system must be cost effective, regarding payload, initial investments, operational expenditure and long-term maintenance costs, while being able to provide the necessary station keeping ability to the floating unit, resisting to current, wind and wave loads, from mild to harsh environmental conditions.

During a FOWT project, the mooring system stiffness has to be specified and designed in accordance with a set of static and dynamic criteria. In essence, the mooring stiffness has to be high enough to keep the unit offset within operational margins, whereas detuning its dynamics from slow-drift forces due to the action of waves and wind in the presence of ocean currents. Such a task is usually accomplished through integrated nonlinear numerical simulations, in which the whole system, including the mooring lines, is modeled from

the point of view of hydrodynamics, aerodynamics and dynamics. Quite sophisticated linear and nonlinear codes are available nowadays; see, e.g. [1]. Nonetheless, in early stages of a complex project, expedite tools are always useful. This is the case regarding a preliminary specification of a proper mooring system stiffness matrix in the horizontal plane.

Using classic approaches of analytical mechanics, this paper addresses the general problem and provides an analytic and explicit formulation for the horizontal plane stiffness matrix of a generic mooring system layout. This is done around a generic offset position and heading of the floating unit, given the curves of tension for each mooring line as nonlinear functions of the displacement of the respective fairlead on the horizontal plane. Possible friction with the seabed is neglected. From basic concepts of mechanics, the problem is formulated in a general way, by deriving the stiffness matrix from generalized mooring forces associated to a set of generalized displacements on the horizontal plane. Then, around any configuration, a stiffness matrix is obtained locally and analytically, for a generic mooring layout. In the formulation, coupling stiffness terms are clearly revealed, whereas the effect of local tension is made explicit.

The international benchmark of the Offshore Code Comparison Collaboration Continuation – OC4 is taken as a case study. The use of the analytical formulation is exemplified by systematically varying the mean offset position and heading of the platform, as well as the pre-tensioning of the mooring system. Colored maps for the stiffness matrix are plotted, where symmetric and antisymmetric patterns are disclosed. Finally, an assessment on the eigenvalue problem as a function of position and heading is made, exemplified by maps of natural periods and illustrated with the corresponding oscillation modes.

THE STIFFNESS MATRIX MODEL

Consider a generic moored body, as sketched in Figure 1. As we are mostly interested in the mooring stiffness on the horizontal plane, the problem is taken as planar. All fairlead mooring line positions, P_i , $i=1, \dots, N$, are supposed to pertain to the same horizontal plane, say α , which is taken as the plane of motion. Let Oxy and $G\xi\eta$ be two reference frames where, for convenience, G is the projection of the position of the center of mass of the body onto the considered plane of motion, α . The frame Oxy , oriented by the unity vectors (\vec{i}, \vec{j}) and defined with the origin at the equilibrium position of the autonomous system, is grounded to the earth. $G\xi\eta$ is a moving frame, fixed to the body. Let A_i be the projection of the anchor position of a particular mooring line, i , onto α , such that $r_i = \overline{A_i P_i} = |A_i - P_i|$. Let also $l_i = \overline{P_i G} = |P_i - G|$ be the distance between P_i and G and β_i the angle formed by $\overline{P_i G}$ with respect to the axis $G\xi$.

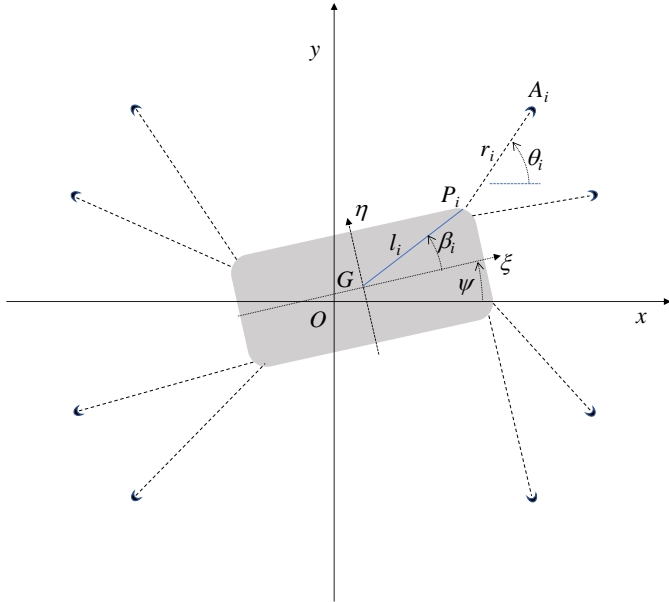


Figure 1: Sketch of a horizontal plan view of a generic moored body at a generic offset position and heading. The projection onto the plane of motion α is detailed for a particular mooring line $i=1, \dots, N$.

Define $\mathbf{q} = [u \ v \ \psi]^T$ as the generalized coordinate vector that gives the position of the body with respect to the fixed frame. The displacements $(u, v) = (x_G, y_G)$ are the Cartesian coordinates of G and ψ is the heading angle with respect to Ox . Each fairlead position P_i may be then written as a function $P_i = P_i(\mathbf{q})$, in the form:

$$(P_i - O) = (u + l_i \cos(\psi + \beta_i))\vec{i} + (v + l_i \sin(\psi + \beta_i))\vec{j} \quad (1)$$

For each mooring line, define also the directional unity vector, $\vec{e}_i = \vec{e}_i(\mathbf{q})$,

$$\vec{e}_i = \frac{(A_i - P_i)}{|A_i - P_i|} = \cos \theta_i \vec{i} + \sin \theta_i \vec{j} \quad , \quad (2)$$

where

$$\begin{aligned} \cos \theta_i &= \frac{(x_{A_i} - x_{P_i})}{r_i} = \frac{(x_{A_i} - (u + l_i \cos(\psi + \beta_i)))}{r_i} \\ \sin \theta_i &= \frac{(y_{A_i} - y_{P_i})}{r_i} = \frac{(y_{A_i} - (v + l_i \sin(\psi + \beta_i)))}{r_i} \end{aligned} \quad (3)$$

with

$$r_i^2 = (x_{A_i} - (u + l_i \cos(\psi + \beta_i)))^2 + (y_{A_i} - (v + l_i \sin(\psi + \beta_i)))^2 \quad (4)$$

Notice that r_i and θ_i are both functions of \mathbf{q} . Neglecting a possible effect of friction with the seabed, consider now that each mooring line will contribute with the horizontal component of a restoring force applied to the vessel, in the form,

$$\vec{F}_i = \vec{F}_i(r_i) = f_i(r_i)\vec{e}_i, \quad (5)$$

where $f_i(r_i) = f_i(P_i(\mathbf{q}); A_i) = f_i(\mathbf{q})$ is a nonlinear function of the distance $r_i = \overline{A_i P_i} = |A_i - P_i|$ that characterizes each mooring line. Notice that such a function should be known a priori and may represent from a simple catenary line to a composed and extensible line made of various segments, as chain and ropes. The way the functions are constructed can vary from analytical methods, for the simple catenary case, to numerical ones. Such functions might also take into account the action of sea current, although this point is left for a further paper. An example for a simple catenary line is given in the Appendix.

From the classical methods of analytical mechanics, the corresponding generalized restoring force vector, $\mathbf{Q} = [Q_u \ Q_v \ Q_\psi]^T$, is then supposed to be a function of the position \mathbf{q} only, in a quasi-static approach. For conciseness sake, let Q_j , $j=1, 2, 3$ designate the generalized restoring forces for (u, v, ψ) , respectively. Then, from any good textbook of analytical mechanics, e.g., [1], [3],

$$Q_j = \sum_{i=1}^N \vec{F}_i \cdot \frac{\partial P_i}{\partial q_j} = \sum_{i=1}^N f_i(r_i)\vec{e}_i \cdot \frac{\partial P_i}{\partial q_j} = -\frac{\partial V}{\partial q_j} \quad , \quad (6)$$

where $V = V(\mathbf{q}; \Pi)$ is defined as the mooring system force potential function, being $\Pi = \{(A_i, l_i, \beta_i); i=1, \dots, N\}$ the set of geometric parameters. In the jargon of analytical mechanics, $\partial P_i / \partial q_j$ is sometimes referred to as the local generalized direction corresponding to q_j . Locally, around any chosen configuration \mathbf{q} , the mooring system stiffness matrix $\mathbf{K}(\mathbf{q})$ may be then determined, as the Hessian of $V = V(\mathbf{q}; \mathbf{p}_i)$. In fact,

$$\mathbf{K}(\mathbf{q}) = \left[\frac{\partial^2 V}{\partial q_j \partial q_k} \right] = - \left[\frac{\partial Q_j}{\partial q_k} \right], \quad (7)$$

From (6), it follows then that,

$$\begin{aligned}
K_{jk} &= -\frac{\partial}{\partial q_k} \sum_{i=1}^N f_i(r_i) \bar{e}_i \cdot \frac{\partial P_i}{\partial q_j} = \\
&= -\sum_{i=1}^N \frac{\partial f_i}{\partial q_k} \bar{e}_i \cdot \frac{\partial P_i}{\partial q_j} - \sum_{i=1}^N f_i \frac{\partial}{\partial q_k} \left(\bar{e}_i \cdot \frac{\partial P_i}{\partial q_j} \right) = \\
&= -\sum_{i=1}^N f_i' \frac{\partial r_i}{\partial q_k} \bar{e}_i \cdot \frac{\partial P_i}{\partial q_j} - \sum_{i=1}^N f_i \left(\frac{\partial \bar{e}_i}{\partial q_k} \cdot \frac{\partial P_i}{\partial q_j} + \bar{e}_i \cdot \frac{\partial^2 P_i}{\partial q_k \partial q_j} \right)
\end{aligned} \tag{8}$$

where

$$f_i' = df_i/dr_i = k_i(r_i) \tag{9}$$

is the local horizontal stiffness of the i -th mooring line. Notice that in the second summation term in Eq. (8), the effect of the horizontal component of the tension, $f_i(r_i) = f_i(\mathbf{q})$, of each mooring line at that position, appears explicitly. Notice that Eq. (8) is general indeed, seen the assumed hypotheses. Notice also that this matrix is a local linearization of the system nonlinear stiffness, at any assumed configuration, i.e., at any mean dislocation of the vessel that might be caused by the environmental forces. Addressing the problem of finding such mean equilibrium position under environmental forces is not in the scope of the present paper and shall be discussed in a further work, for completeness sake.

After some straightforward algebra (see Appendix A), and defining

$$\bar{k}_i(r_i) = f_i(r_i)/r_i \tag{10}$$

as the ‘string stiffness’, i.e., that associated to the tensioning of each mooring line at a given position \mathbf{q} , we finally arrive at a symmetric stiffness matrix for the moored system,

$$\mathbf{K}(\mathbf{q}) = \begin{bmatrix} k_{uu} & k_{uv} & k_{u\psi} \\ k_{uv} & k_{vv} & k_{v\psi} \\ k_{u\psi} & k_{v\psi} & k_{\psi\psi} \end{bmatrix} \tag{11}$$

where

$$\begin{aligned}
k_{uu} &= \sum_{i=1}^N \left(k_i \cos^2 \theta_i + \bar{k}_i \sin^2 \theta_i \right) \\
k_{vv} &= \sum_{i=1}^N \left(k_i \sin^2 \theta_i + \bar{k}_i \cos^2 \theta_i \right) \\
k_{\psi\psi} &= \sum_{i=1}^N \left(k_i l_i^2 \sin^2(\psi + \beta_i - \theta_i) \right) + \\
&\quad + \sum_{i=1}^N \bar{k}_i l_i^2 \left(\cos^2(\psi + \beta_i - \theta_i) + \frac{r_i}{l_i} (\cos(\psi + \beta_i - \theta_i)) \right)
\end{aligned} \tag{12}$$

and

$$\begin{aligned}
k_{uv} &= k_{vu} = \sum_{i=1}^N (k_i - \bar{k}_i) \sin \theta_i \cos \theta_i \\
k_{u\psi} &= k_{\psi u} = -\sum_{i=1}^N (k_i l_i \cos \theta_i \sin(\psi + \beta_i - \theta_i)) + \\
&\quad + \sum_{i=1}^N (\bar{k}_i l_i \sin \theta_i \cos(\psi + \beta_i - \theta_i)) \\
k_{v\psi} &= k_{\psi v} = -\sum_{i=1}^N (k_i l_i \sin \theta_i \sin(\psi + \beta_i - \theta_i)) + \\
&\quad + \sum_{i=1}^N (\bar{k}_i l_i \cos \theta_i \cos(\psi + \beta_i - \theta_i))
\end{aligned} \tag{13}$$

The effect of the ‘string stiffness’, $\bar{k}_i(r_i)$, is analogous to that of a tensioned string in a perpendicular direction to its axis, as in a violin chord, for instance. The presence of terms related to \bar{k}_i can be of crucial importance, particularly to the yawing rigidity, for some symmetric mooring arrangements with a central point, as those used in an equilateral triangular semi-submersible platform, for example. Such an issue will be explored in the next section. Notice that the ‘string stiffness’ terms have sometimes been missed in the specialized technical literature; see, e.g., [4], page 266, Eq. (8.26). As a matter of fact, stiffness matrices for systems composed by inclined linear springs may be found in many textbooks; see, e.g., [5], p 572-576. However, the ‘spring stiffness’ effect on the torsional stiffness (the yawing stiffness in the present case) is not so commonly found. Formulations for generic restoring force functions are not commonly found either.

Observe also that, would the reader prefer to work on the vessel reference frame, $G\xi\eta$, a simple rotation should be applied in the form,

$$\hat{\mathbf{K}} = \mathbf{B} \mathbf{K} \mathbf{B}^t, \tag{14}$$

where

$$\hat{\mathbf{K}} = \begin{bmatrix} k_{\xi\xi} & k_{\xi\eta} & k_{\xi\psi} \\ k_{\xi\eta} & k_{\eta\eta} & k_{\eta\psi} \\ k_{\xi\psi} & k_{\eta\psi} & k_{\psi\psi} \end{bmatrix}, \tag{15}$$

and

$$\mathbf{B} = \begin{bmatrix} \cos \psi & \sin \psi & 0 \\ -\sin \psi & \cos \psi & 0 \\ 0 & 0 & 1 \end{bmatrix}, \tag{16}$$

Certainly, the same general result could have been derived through perturbation techniques, by retaining first order terms in $(\delta u, \delta v, \delta \psi)$ in the Taylor series expansions of the mooring line horizontal force functions, around any given position, (u, v, ψ) , as originally done in [6]; see also [5]. However, approaching the problem through the methods of analytical mechanics, besides much more elegant, produces concise, straightforward and general results, concerning the use of any

suitable nonlinear restoring force function $f_i(r_i) = f_i(P_i(\mathbf{q}); A_i) = f_i(\mathbf{q})$. Moreover, the generalized forces given in Eq. (6) may be applied in nonlinear analysis procedures or in direct nonlinear dynamic numerical simulations.

CASE STUDY: THE OC4 FOWT

To illustrate and discuss the application of the analytical method, we take the OC4-DeepCwind, semi-submersible type, Floating Offshore Wind Turbine, [8], as a case of study. The mooring line arrangement is supposed to be triangular equilateral, as shown in Figure 2. Table 1 shows the relevant data for the analysis of the chosen moored system.

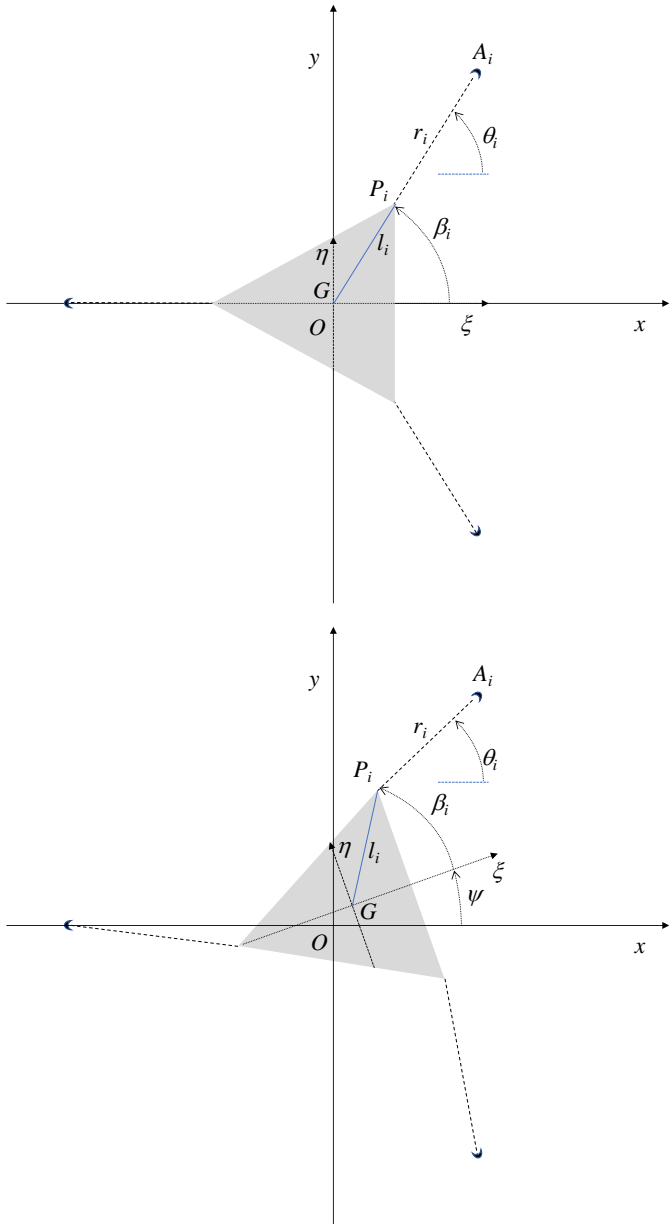


Figure 2: An equilateral triangular mooring system arrangement.

Obviously, for such a symmetric arrangement and under no external force, the equilibrium position of the system is the trivial one, $\mathbf{q} = [0 \ 0 \ 0]^T = \mathbf{0}$.

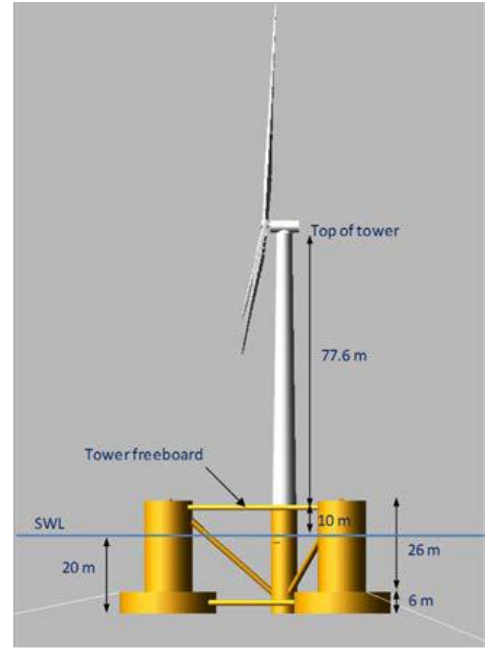


Figure 3: The OC4-DeepCwind floating wind system; illustration extracted from [7].

Table 1. OC4-DeepCwind Semi-Submersible Floating Offshore Wind Turbine platform and mooring system relevant data; [7][8]

FOWT unity	
Type	Semi-sub
Mass	14,267 t
Yaw moment of inertia around G_z	12.260E06 tm^2
Surge added mass ($M_{a\xi\xi}$) ^(*)	8,270 t
Sway added mass ($M_{a\eta\eta}$) ^(*)	8,270 t
Yaw added moment of inertia ($I_{a\psi\psi}$) ^(*)	6.230E06 tm^2
Center of mass (G)	centered
Draught	20 m
Diameter of central column	6.5 m
Diameter of offset columns	12 m
Diameter of base columns	24 m
Diameter of braces	1.6 m
(*) at zero frequency	
Mooring system	
Number of mooring lines	3
Type	mooring chain
Equidistant arrangement	at 120°
Radius from center to anchors ($\overline{A_i 0}$)	837.6m
Radius from center to fairleads (l)	40.9m
Mass per unit length (μ)	113.35kg/m
Immersed weight per unit length (γ)	1064.6N/m
Unstretched mooring length (base case) (L)	835.5m
Horizontal pre-tension (base case)	962.57kN

Moreover, at the trivial equilibrium position we have $\beta_i = \theta_i, i=1,2,3$, so that the first summation in the yaw stiffness coefficient, $k_{\psi\psi}$, given in Eq. (12) turns to be identically null, as expected.

The second summation term is not null, though. In fact, at $\mathbf{q} = \mathbf{0}$, with $r_i = r, l_i = l$ and $\bar{k}_i(r_i) = f_i(r_i)/r_i = \bar{k}, i=1,2,3$, $k_{\psi\psi}$ reduces to

$$k_{\psi\psi} \Big|_{\mathbf{q}=\mathbf{0}} = \sum_{i=1}^3 \bar{k}_i l_i^2 \left(1 + \frac{r_i}{l_i}\right) = 3\bar{k}l^2 \left(1 + \frac{r}{l}\right) \quad (17)$$

In other words, in this particular configuration, the pure yaw stiffness is only function of the ‘string stiffness’, \bar{k} . If this term is ignored, the analyst might be erroneously led to the conclusion that the yaw stiffnesses would be identically null at the trivial equilibrium position, contradicting any intuitive argument.

For completeness, the reader can easily verify from Eqs. (12) and (13) that, at $\mathbf{q} = \mathbf{0}$, with $k_i(r_i) = f_i(r_i) = k$, the stiffnesses matrix for the triangular arrangement is diagonal and reduces to

$$\mathbf{K}(\mathbf{0}) = \frac{3}{2} \begin{bmatrix} (k + \bar{k}) & 0 & 0 \\ 0 & (k + \bar{k}) & 0 \\ 0 & 0 & 2\bar{k}l^2 \left(1 + \frac{r}{l}\right) \end{bmatrix}. \quad (18)$$

Notice that, generally speaking, the ‘string stiffness’ effect may be indeed significant, not only for such peculiar arrangements and particular configurations. In fact, in a taut-leg mooring system, where pre-tensioning is high and the mooring system radius relatively small, the ‘string stiffness’ may become even more relevant. The same may be also true for systems composed by mixed mooring lines, with chain and ropes. Such an issue is left for a further paper.

From now on, attention is given to the OC4-DeepCwind FOWT mooring system, focusing on the effect of pre-tensioning on the stiffness matrix and on the natural periods of the motions in the horizontal plane. A simple catenary model is taken to compute the horizontal restoring force function $f_i(r_i)$, since for chains the geometric rigidity is much lower than the elastic one, in general. This is the case for the system under study. The catenary model for $f_i(r_i)$ is given in the appendix. Pre-tensioning is defined at the trivial equilibrium position. The design condition, corresponding to the data given in Table 1, is taken as the base case. Two other pre-tensioning conditions are analyzed: a ‘low’ one, with pretension reduced by 10% and a ‘high’ one, with pretension augmented by 10%. Table 2 presents the corresponding unstretched mooring line lengths and respective pre-tensioning values.

Figure 4 shows a colored map of the stiffness matrix coefficients for the design condition, as functions of the displacement of the center of mass of the platform from the trivial equilibrium position.

Table 2. OC4-DeepCwind mooring system analyzed conditions

Pre-tensioning condition	Low	Design	High
Pre-tensioning ratio (f*) w.r.t design	0.9	1.0	1.1
Unstretched mooring line length (m)	837.0	835.5	833.5
Horizontal pre-tensioning (kN)	866.3	962.6	1058.8
Pre-tensioning (kN)	1079.1	1161.0	1266.4
Angle at fairlead w.r.t. horizontal (°)	35.3	34.0	32.5

Values are given in kN and m. This is done for a single heading angle, $\psi = 0^\circ$, taking displacements $u^* = u/l$ and $v^* = v/l$ in the interval $[-0.25, +0.25]$. In other words, these maps present the elements of $\mathbf{K}(u, v, 0)$. It should be observed the large variability of all coefficients within the considered interval. Symmetric and anti-symmetric patterns are also shown explicitly. Notice, for instance, the symmetry of the elements in the diagonal, with respect to the displacement v , as should be expected. On the other hand, the off-diagonal terms, k_{uv} and $k_{\psi\psi}$, are respectively anti-symmetric and symmetric with respect to v , whereas $k_{u\psi}$ is anti-symmetric w.r.t. to both, u and v . For this symmetric heading condition ($\psi = 0^\circ$), such qualitative results could have been intuitively anticipated and may be observed from Eqs. (12) and (13).

Figure 5 repeats the same results of Figure 4, however in a different color scale. This change in scale is made for direct comparisons with other cases, presented in Figs. 6-10. The color scales are preserved hereinafter. Figure 6 illustrates how a relatively small heading angle, chosen illustratively as $\psi = 10^\circ$, may affect the stiffness matrix. Compared to the base case, the diagonal terms reveal some increasing. Changes are more pronounced for the off-diagonal terms, particularly to those involving the heading angle. The coupled terms reveal the existence of some symmetry (anti-symmetry) breakings. Figures 7 to 10 illustrate how pre-tensioning affects the stiffness matrix. Figures 7 and 8 treat a case in which the pre-tensioning of the design case has been reduced by 10%. Both heading angles are considered, for comparison sake. Though small, quantitative changes are perceptible. The qualitative behavior remains the same, as can be seen by comparing Figs. 7 and 5 and Figs. 8 and 6. The same kind of symmetries and anti-symmetries are observed in Fig. 7, as well the same symmetry / anti-symmetry breakings in Fig. 8, caused by a non-symmetric heading. On the other hand, by increasing pre-tensioning by 10%, the stiffness is augmented significantly, as neatly shows the diagonal terms of Figures 9 and 10.

With a quantitative analysis purpose, Table 3 presents numerical values for some of the conditions at null heading ($\psi = 0^\circ$). For concision, only the design pre-tensioning condition is exemplified. The mentioned symmetries and anti-symmetries with respect to the displacements u^* and v^* are now quantitatively explicit, much more than could be revealed by the colored maps. Table 4 refers to the same pre-tensioning design condition, but at a small heading angle, ($\psi = 10^\circ$). Symmetry and anti-symmetry breakings due to the non-null heading angle are noticeable.

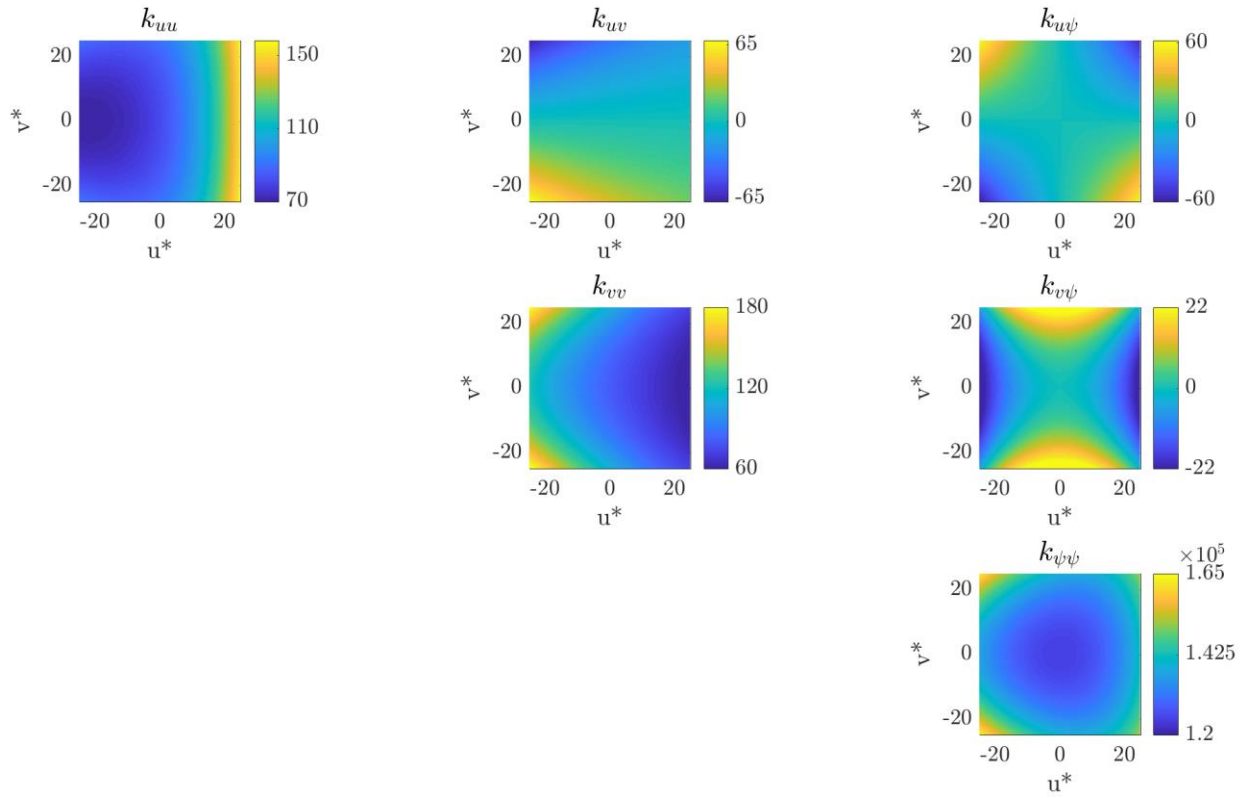


Figure 4: OC-4 DeepCwind FOWT. Stiffness Matrix coefficients as function of displacements, in percentage of $l = 40.9\text{m}$. Heading: $\psi = 0^\circ$. Base case. Pre-tensioning: design conditions. Pre-tensioning ratio: $f^*=1.0$. Unities: kN and m. Amplified color scales.

Table 3. OC4-DeepCwind mooring system stiffness matrix; $\psi = 0^\circ$. Design pre-tensioning case. Units in kN and m.

$(u^*, v^*) = (0, 0)$		
81,25	0,00	0,00
	81,25	0,00
		1,24E+05
$(u^*, v^*) = (0.25, 0.25)$		
157,93	-19,81	-58,91
	71,94	-3,20
		1,52E+05
$(u^*, v^*) = (-0.25, 0.25)$		
90,71	-68,27	61,38
	183,24	-4,68
		1,64E+05
$(u^*, v^*) = (0.25, -0.25)$		
157,93	19,81	58,91
	71,94	-3,20
		1,52E+05
$(u^*, v^*) = (-0.25, -0.25)$		
90,71	68,27	-61,38
	183,24	-4,68
		1,64E+05

Table 4. OC4-DeepCwind mooring system stiffness matrix; $\psi = 10^\circ$. Design pre-tensioning case. Units in kN and m

$(u^*, v^*) = (0, 0)$		
85,28	0,00	0,00
	85,28	0,00
		1,36E+05
$(u^*, v^*) = (0.25, 0.25)$		
167,33	-22,33	648,91
	76,75	371,96
		1,68E+05
$(u^*, v^*) = (-0.25, 0.25)$		
94,95	-72,63	-700,68
	197,07	1113,17
		1,84E+05
$(u^*, v^*) = (0.25, -0.25)$		
170,47	19,99	793,89
	74,76	-380,33
		1,70E+05
$(u^*, v^*) = (-0.25, -0.25)$		
98,04	75,30	-850,07
	195,14	-1124,58
		1,85E+05

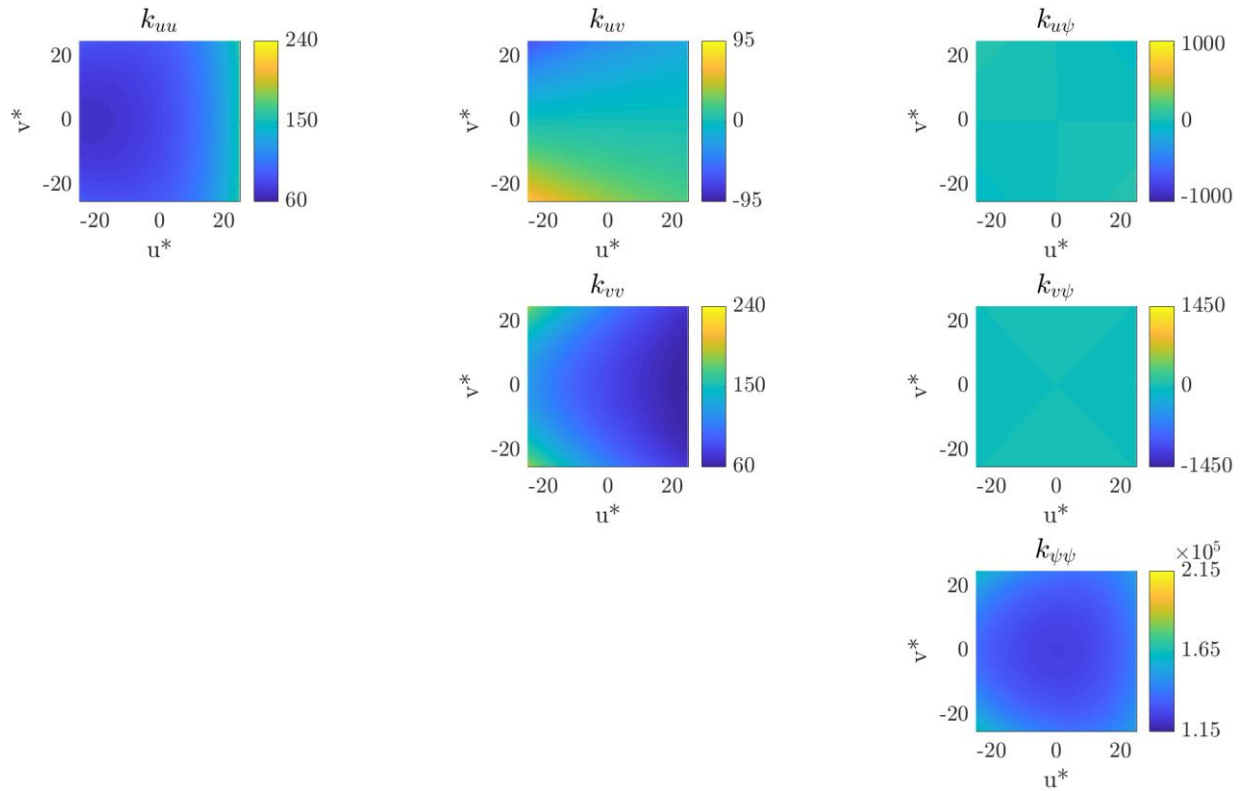


Figure 5: OC-4 DeepCwind FOWT. Stiffness Matrix coefficients as function of displacements, in percentage of $l = 40.9\text{m}$. Heading: $\psi = 0^\circ$. Base case. Pre-tensioning: design conditions. Pre-tensioning ratio: $f^*=1.0$. Unities: kN and m.

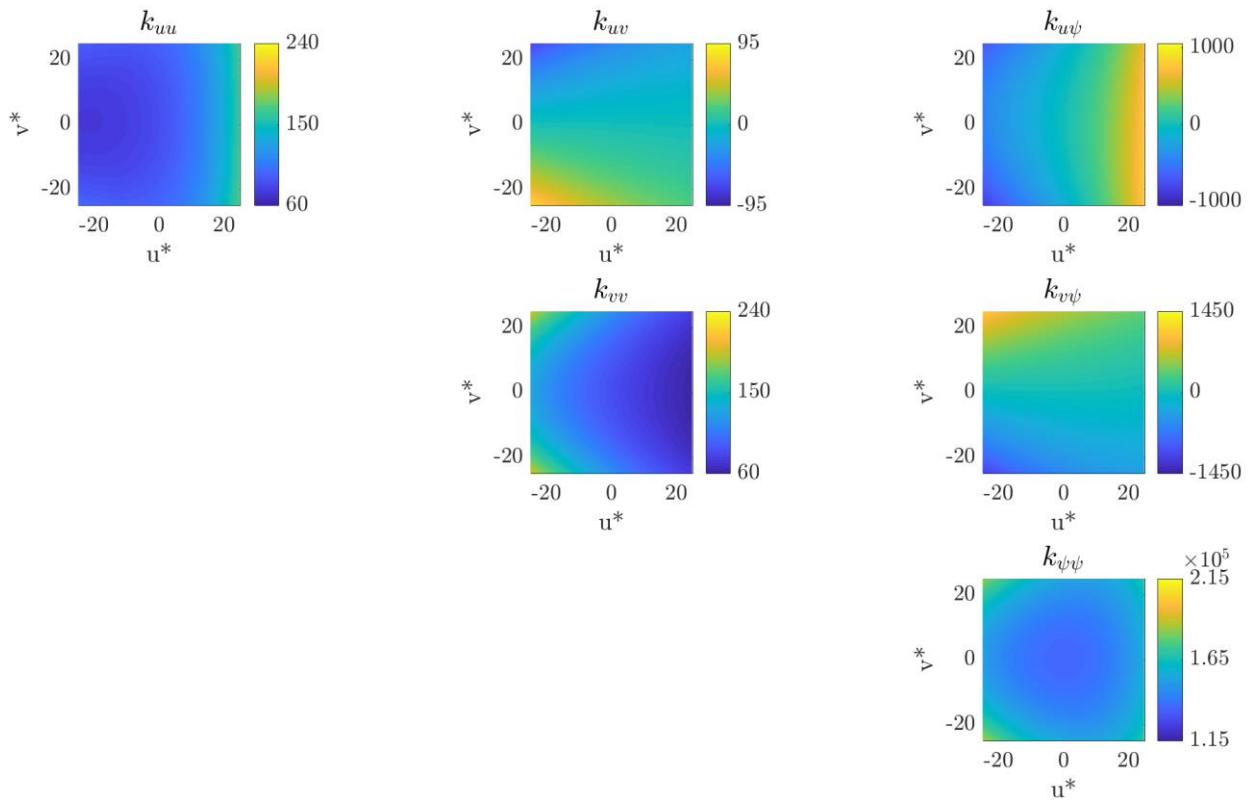


Figure 6: OC-4 DeepCwind FOWT. Stiffness Matrix coefficients as function of displacements, in percentage of $l = 40.9\text{m}$. Heading: $\psi = 10^\circ$. Base case. Pre-tensioning: design conditions. Pre-tensioning ratio: $f^*=1.0$. Unities: kN and m.

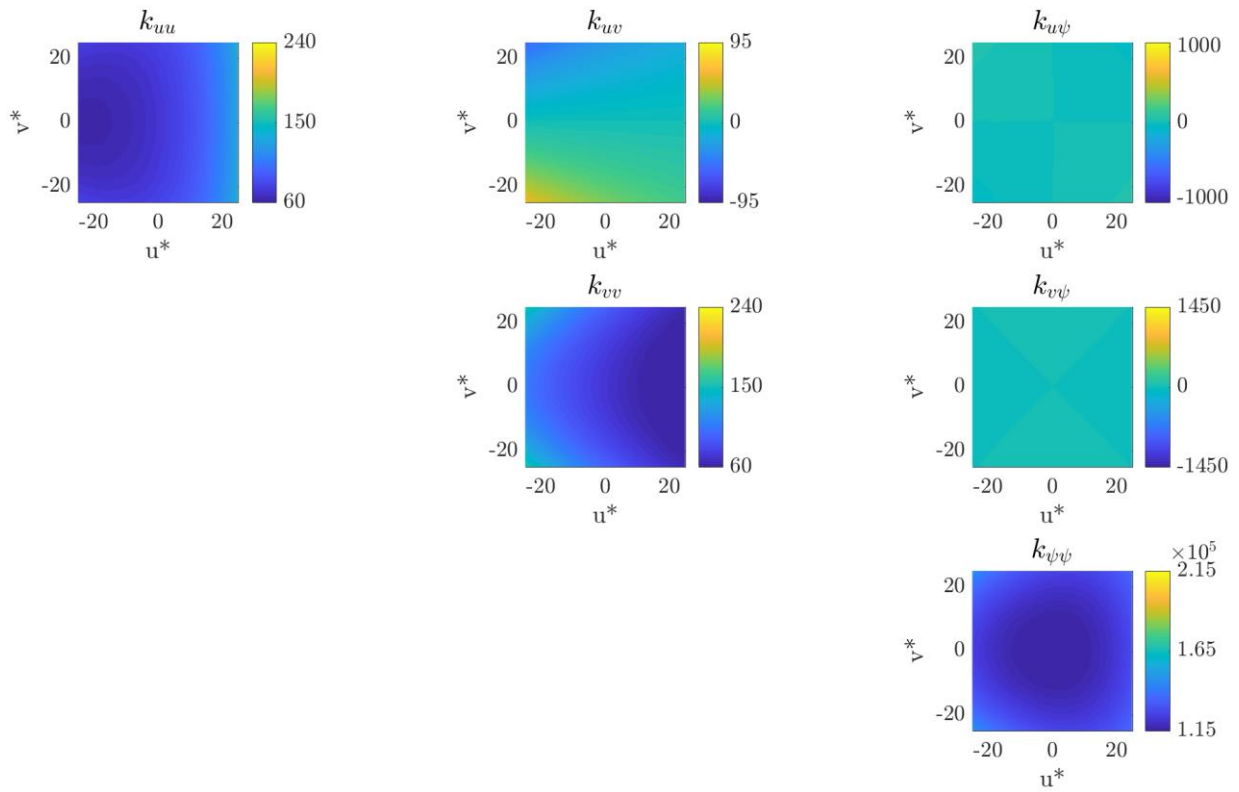


Figure 7: OC-4 DeepCwind FOWT. Stiffness Matrix coefficients as function of displacements, in percentage of $l = 40.9\text{m}$. Heading: $\psi = 0^\circ$. ‘Low’ pre-tensioning: case. Pre-tensioning ratio: $f^*=0.9$. Unities: kN and m.

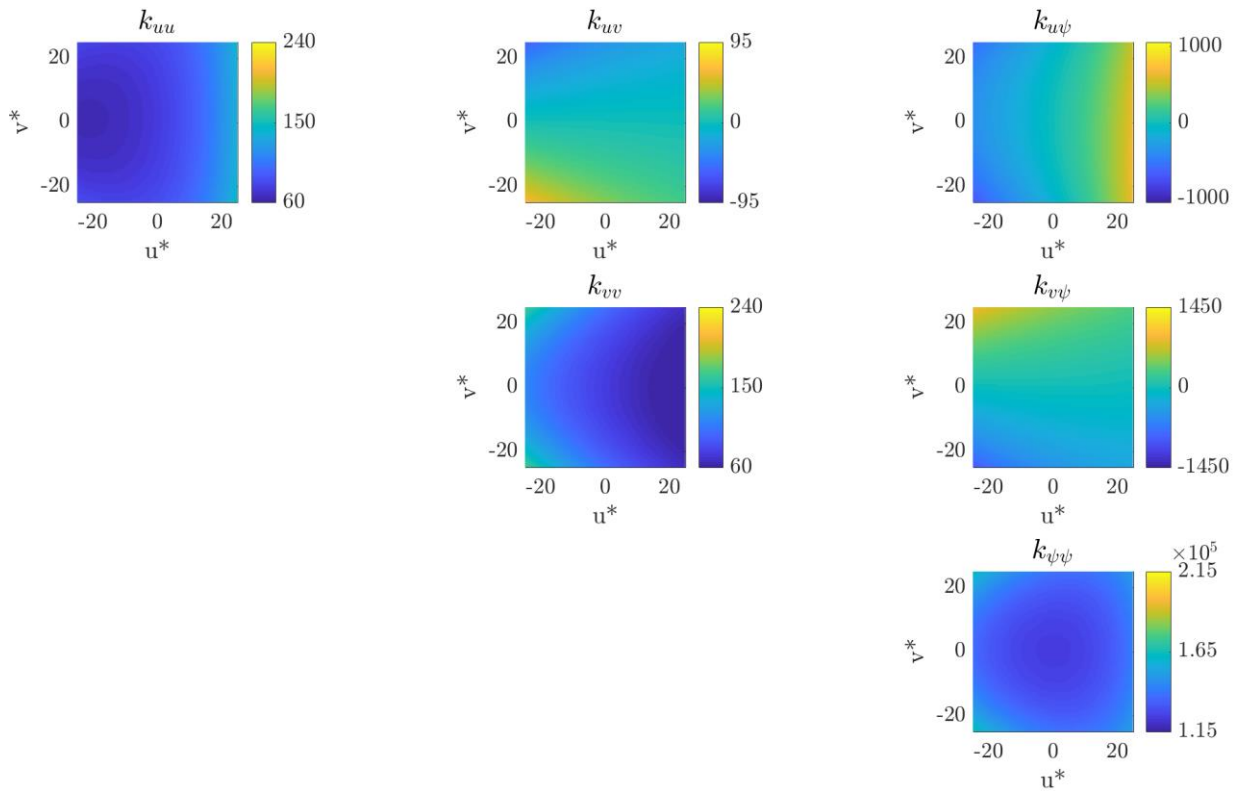


Figure 8: OC-4 DeepCwind FOWT. Stiffness Matrix coefficients as function of displacements, in percentage of $l = 40.9\text{m}$. Heading: $\psi = 10^\circ$. ‘Low’ pre-tensioning: case. Pre-tensioning ratio: $f^*=0.9$. Unities: kN and m.

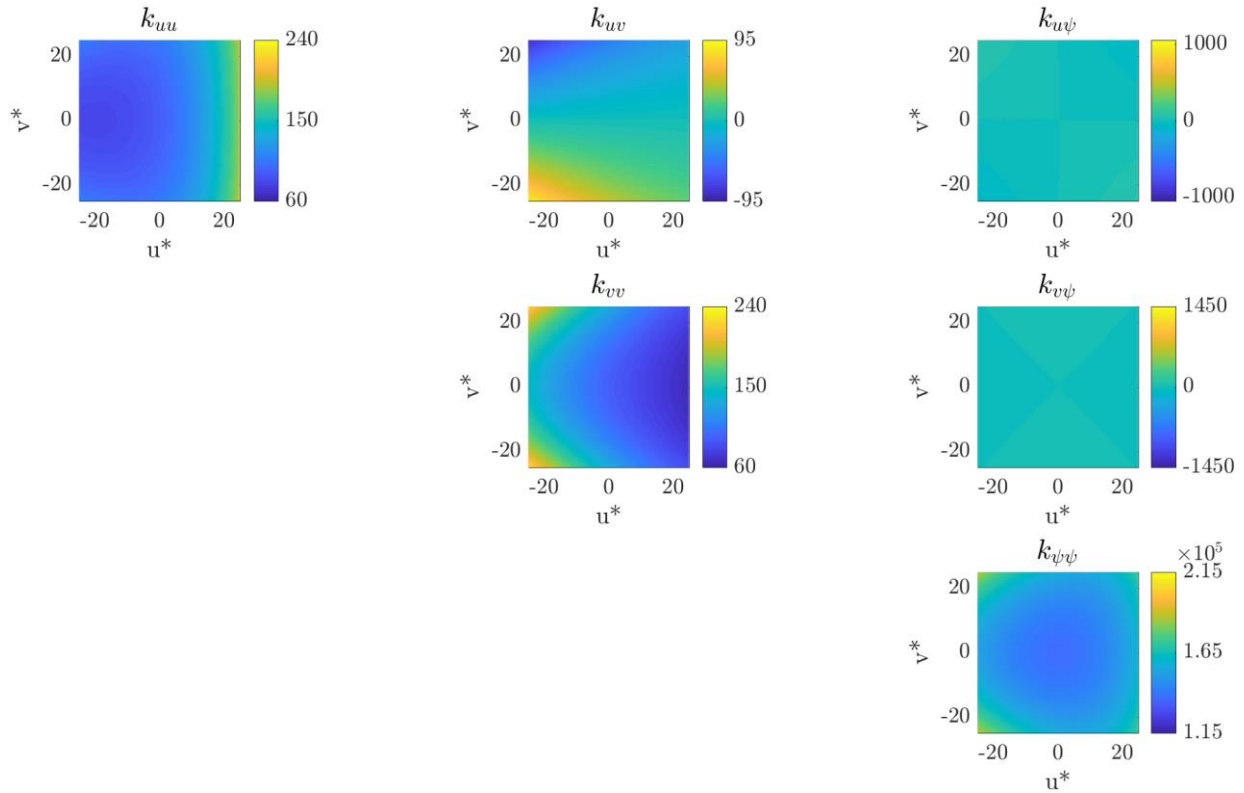


Figure 9: OC-4 DeepCwind FOWT. Stiffness Matrix coefficients as function of displacements, in percentage of $l = 40.9\text{m}$. Heading: $\psi = 0^\circ$. ‘High’ pre-tensioning: case. Pre-tensioning ratio: $f^*=1.1$. Unities: kN and m.

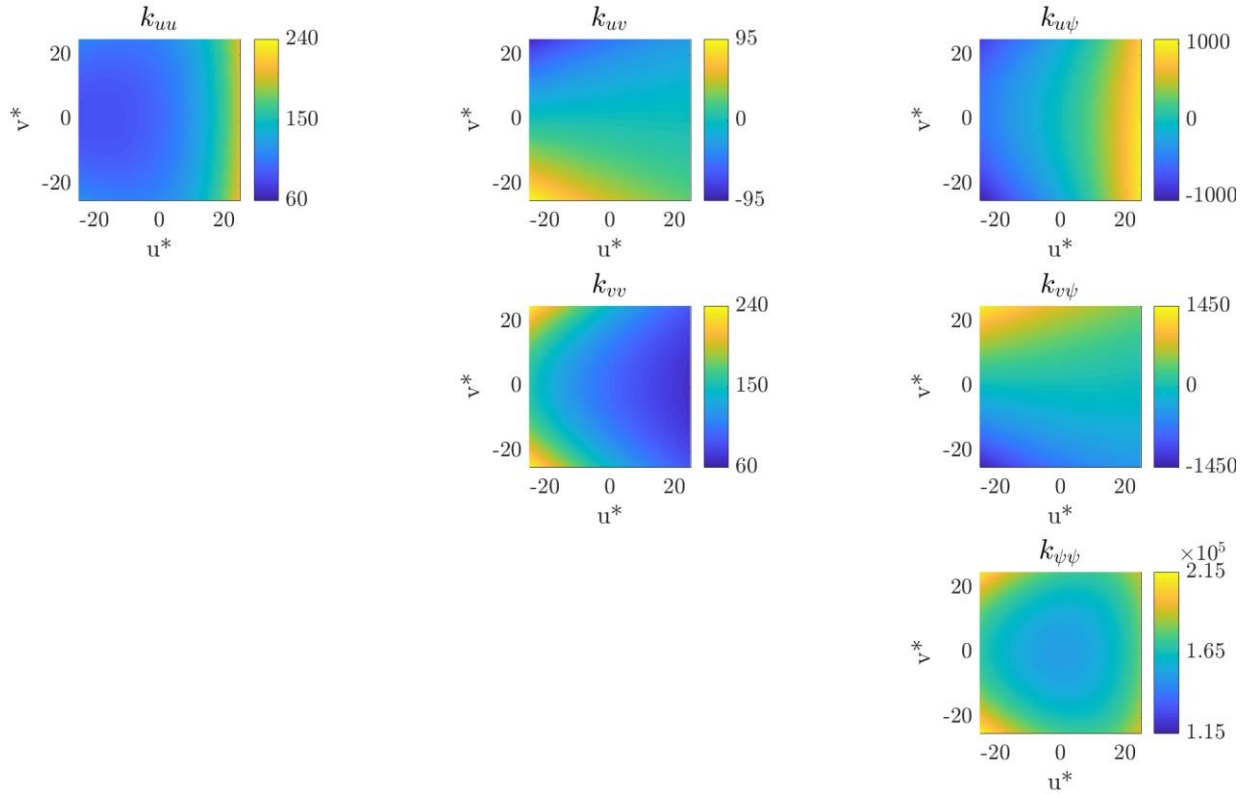


Figure 10: OC-4 DeepCwind FOWT. Stiffness Matrix coefficients as function of displacements, in percentage of $l = 40.9\text{m}$. Heading: $\psi = 10^\circ$. ‘High’ pre-tensioning: case. Pre-tensioning ratio: $f^*=1.1$. Unities: kN and m.

At last, an assessment on how the mean position of the platform may influence the natural periods and modes of oscillation is made. A classic linear eigenvalue problem is solved within the same intervals of displacements u^* and v^* , for the headings $\psi=0^\circ$ and $\psi=10^\circ$. For that, added masses and moment of inertia have been determined through a worldwide-recognized panel method-based software, [9]. Figure 11 shows the added masses and moment of inertia, $(M_{a\xi\xi}; M_{a\eta\eta}; I_{a\psi\psi})$, in surge, sway and yaw, as function of the period of oscillation. As well known, these added inertia coefficients tend to asymptotic values as the oscillation periods go to infinity. Such asymptotic values may then be taken as representative ones for a first estimate of (large) natural periods in the horizontal plane.

It has to be noticed that in the asymptotic limit of zero-frequency, the motions on the horizontal plane could have been considered under a double-body modelling in an infinite fluid, thus under no free-surface effects. Moreover, regular polygonal shaped bodies, therefore polygonal symmetric, have equal added masses in orthogonal directions, i.e., $M_{a\xi\xi} = M_{a\eta\eta}$; see, e.g., [10], page 37. In other words, in the present case, the added mass matrix, besides diagonal, is invariant with respect to a planar rotation, ψ , as that considered in this paper, such that $M_{a uu} = M_{a vv} = M_{a \xi\xi} = M_{a \eta\eta}$. This fact simplifies the numerical work even more in the present case study.

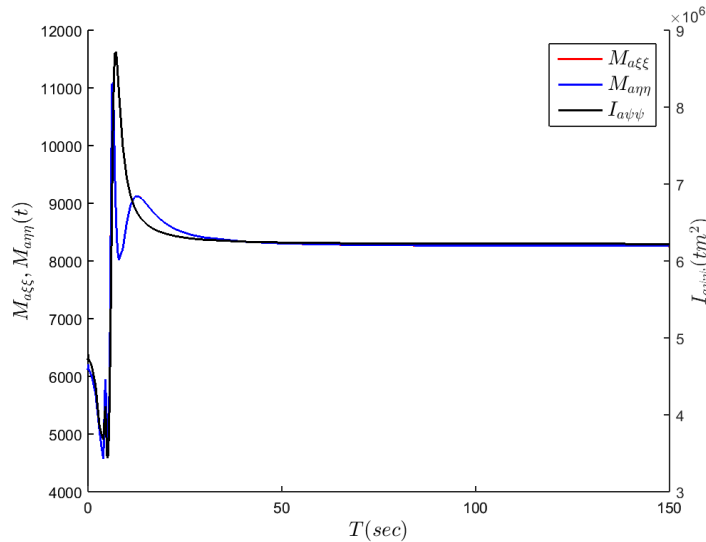


Figure 11: Added masses and moment of inertia as function of period. Determined with WAMIT®; [9].

Figures 12 and 13 present colored maps of the natural periods as function of the position of the center of mass, for $\psi=0^\circ$ and $\psi=10^\circ$. Center lines refer to the design pre-tensioning case; upper lines to the ‘low’ pre-tensioning case and bottom lines to the ‘high’ pre-tensioning one. Natural periods vary from 60 to 120s.

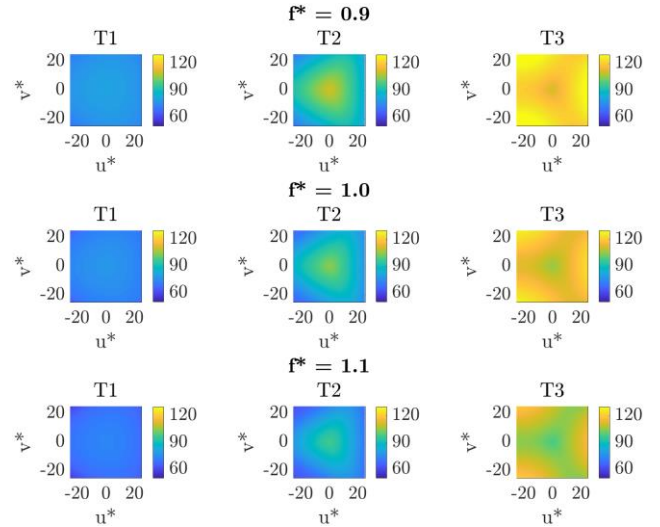


Figure 12: OC-4 DeepCwind FOWT. Natural periods (seconds) as function of pre-tensioning ratio: upper: 0.9; center: 1.0; bottom: 1.1. Heading: $\psi=0^\circ$.

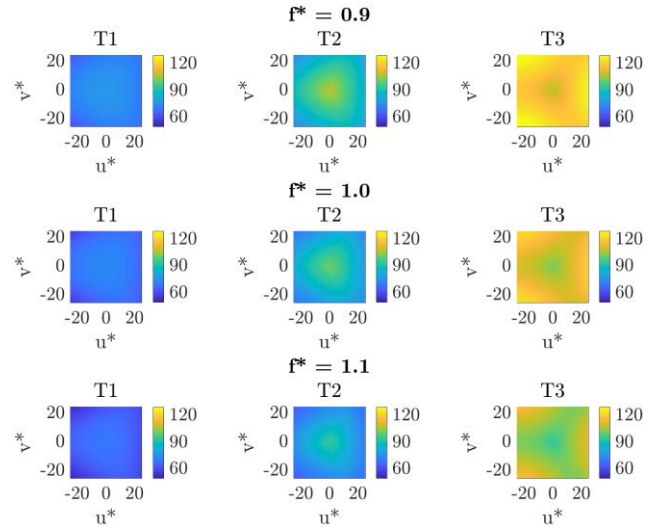


Figure 13: OC-4 DeepCwind FOWT. Natural periods (seconds) as function of pre-tensioning ratio: upper: 0.9; center: 1.0; bottom: 1.1. Heading: $\psi=10^\circ$.

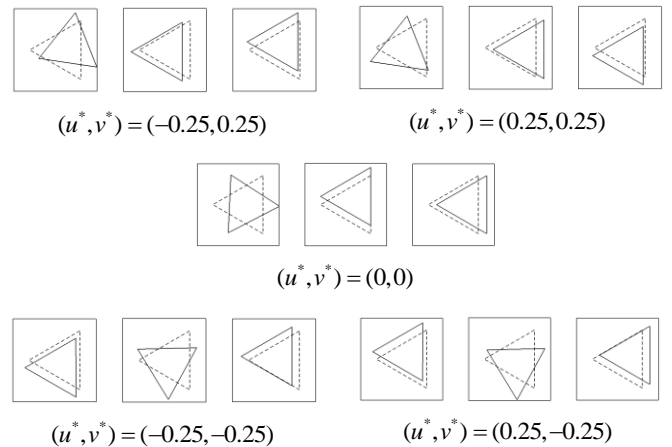


Figure 14: OC-4 DeepCwind. Oscillation modes, corresponding to natural periods, T_j , $j=1,2,3$. Design pre-tensioning case; $f^*=1.0$. $\psi=0^\circ$, Figure 12, center line.

CONCLUSIONS

A simple analytical model has been worked out to deal with the problem of determining the stiffness matrix of a generic mooring system in the horizontal plane, by considering a frictionless seabed. Supported on usual relations of analytical mechanics, from which the generalized mooring forces are constructed, this paper has as main contribution explicit mathematical forms for all the stiffness matrix elements, determined at any mean position the vessel might assume on the horizontal plane. Besides the geometry of the mooring system, the only data needed are the functions that relate the restoring horizontal force of each mooring line to the horizontal projection of the distance between the anchor and the respective fairlead position. Therefore, the procedure is general, in a quasi-static sense, since such functions are to be computed a priori, given the type of each mooring line. Notice that all types of mooring lines may be accounted for, from simple catenary lines to mixed ones.

A particular practical contribution of the analytical formulation is the discussion on the importance of terms related to the tensioning of the lines (the ‘string stiffness’) at a given position and not only of terms related to the derivatives of the functions of restoring forces with respect to the displacements. Such tensioning terms have sometimes been missing or omitted in the specialized technical literature, e.g., [4], and may have important effects in the case of polygonal arrangements or in very tight mooring systems.

Those aspects have been illustrated through the application of the analytical formulation to the international benchmark of the Offshore Code Comparison Collaboration Continuation – OC4 floating wind turbine. In this particular triangular symmetric arrangement, the yaw stiffness would render exactly null if the ‘string stiffness’ terms were not considered. Finally, the use of the analytical formulae enabled us to construct maps of stiffness as function of the mean offset position of the platform within a certain interval. Symmetries and anti-symmetries with respect to the mean offset of the platform have been revealed through colored maps. The effects of pre-tensioning and heading on the stiffness matrix were also addressed. In particular, how heading may break the alluded symmetric or anti-symmetric patterns. Finally, an assessment on natural periods and respective modes of oscillation varying as function of pre-tensioning, heading and offset position has been made.

The authors believe that this model can contribute practically, if incorporated in the early stages of mooring system design procedures. In fact, being the method analytical, therefore expedite, it may serve as guide for mooring system dimensioning. Further work is envisaged for such an approach towards nonlinear dynamics analysis and bifurcation studies; see, e.g., [11] - [13].

ACKNOWLEDGMENTS

The authors are grateful to Prof. Alexandre N. Simos and Dr. Alfredo Gay Neto, for motivating the present work in the context of the ONRG project nr. N62909-16-1-2066. Thanks also to Eng. Lucas H. S. do Carmo for running WAMIT®. The second author acknowledges an ONRG MSc scholarship; first and third authors refer two CNPq research grants, ns. 308990/2014-5 and 310595/2015-0.

REFERENCES

- [1] Nishimoto, K., Fucatu, Carlos H. “Dynasim - a Time Domain Simulator of Anchored FPSO”. *Journal of Offshore Mechanics and Arctic Engineering*, v. 124, n.4, p. 203-211, 2002.
- [2] Meirovitch, L., “Methods of Analytical Dynamics”, McGraw-Hill, 1988.
- [3] Lanczos, C., “The Variational Principles of Mechanics”, Dover, 1986
- [4] Faltinsen, O.M. “Sea Loads on Ships and Offshore Structures”, Cambridge University Press, 1998.
- [5] Bucalem, M.L., Bathe, K-J, “The mechanics of solids and structures-hierarchical modeling and the finite element solution”. Springer Science & Business Media, 2011.
- [6] Pesce, C.P. “Preliminary Analysis of Moored System Dynamics” (in Portuguese). IPT – Technological Research Institute, Technical Publication no. 77, 1986.
- [7] Robertson, A., Jonkman, J., Masciola, M., Song, H., Goupee, A., Coulling, A., Luan, C. "Definition of the Semisubmersible Floating System for Phase II of OC4". NREL National Renewable Energy Laboratory, Technical Report NREL/TP-5000-60601, 2014.
- [8] Benitz, M.A., Schmidt, D.P., Lackner, M.A., Stewart, G. M. “Comparison of Hydrodynamic Load Predictions Between Engineering Models and Computational Fluid Dynamics for the OC4-DeepCwind Semi-Submersible”, Proc. 33rd International Conference on Ocean, Offshore and Arctic Engineering, San Francisco, California, June 8–13, 2014.
- [9] Lee, C.-H., Newman, J.N. WAMIT® User’s Manual v. 7.061. WAMIT, Inc., 2013.
- [10] Korotkin, A.I., “Added Masses of Ship Structures”, Springer, 2010.
- [11] Bernitsas, M.M., Matsuura, J.P.J., “Revealing Nonlinear Dynamics Phenomena in Mooring Due to Slowly-Varying Drift”. *Journal of Offshore Mechanics and Arctic Engineering*, v. 133 (2), 021302, 2011.
- [12] Kim, B.K., Bernitsas, M.M. “Nonlinear Dynamics and Stability of Spread Mooring with Riser”. *Applied Ocean Research*, v. 23 (2), 111-123, 2001.
- [13] Pesce, C.P., Tannuri, E.A. “Stability and Dynamics of Offshore Single Point Mooring Systems”. *Revista Brasileira de Ciências Mecânicas*, Campinas, v. 19, n.4, p. 531-552, 1997.

APPENDIX

A. Geometric relations

To compute the stiffness matrix coefficients from the general form given by Eq. (8), a set of relations must be worked out. Such relations are easily verifiable by the interested reader, as follows.

(i) ‘Local generalized directions’, $\frac{\partial P_i}{\partial q_j}$; from Eq. (8):

$$\begin{aligned}\frac{\partial P_i}{\partial u} &= \vec{i} \quad ; \quad \frac{\partial P_i}{\partial v} = \vec{j} \\ \frac{\partial P_i}{\partial \psi} &= -l_i (\sin(\psi + \beta_i) \vec{i} - \cos(\psi + \beta_i) \vec{j}) \\ \frac{\partial^2 P_i}{\partial u^2} &= \frac{\partial^2 P_i}{\partial v^2} = \frac{\partial^2 P_i}{\partial u \partial v} = \vec{0} \\ \frac{\partial^2 P_i}{\partial u \partial \psi} &= \frac{\partial^2 P_i}{\partial v \partial \psi} = \vec{0} \\ \frac{\partial^2 P_i}{\partial \psi^2} &= -l_i (\cos(\psi + \beta_i) \vec{i} + \sin(\psi + \beta_i) \vec{j})\end{aligned}\quad . \quad (\text{A.1})$$

(ii) Partial derivatives $\frac{\partial r_i}{\partial q_k}$; from Eqs. (3) and (4):

$$\begin{aligned}\frac{\partial r_i}{\partial u} &= -\cos \theta_i \quad ; \quad \frac{\partial r_i}{\partial v} = -\sin \theta_i \\ \frac{\partial r_i}{\partial \psi} &= l_i \sin(\psi + \beta_i - \theta_i)\end{aligned}\quad . \quad (\text{A.2})$$

(iii) Partial derivatives of the generalized projections of mooring lines unity vectors, $\frac{\partial}{\partial q_k} \left(\vec{e}_i \cdot \frac{\partial P_i}{\partial q_j} \right)$; from Eqs (2), (3), (4), (A.1) and (A.2):

$$\begin{aligned}\frac{\partial}{\partial u} \left(\vec{e}_i \cdot \frac{\partial P_i}{\partial u} \right) &= \frac{\partial}{\partial u} (\cos \theta_i) = -\frac{\sin^2 \theta_i}{r_i} \\ \frac{\partial}{\partial v} \left(\vec{e}_i \cdot \frac{\partial P_i}{\partial v} \right) &= \frac{\partial}{\partial v} (\sin \theta_i) = -\frac{\cos^2 \theta_i}{r_i} \\ \frac{\partial}{\partial u} \left(\vec{e}_i \cdot \frac{\partial P_i}{\partial v} \right) &= \frac{\partial}{\partial u} (\sin \theta_i) = \frac{\sin \theta_i \cos \theta_i}{r_i} = \\ &= \frac{\partial}{\partial v} (\cos \theta_i) = \frac{\partial}{\partial v} \left(\vec{e}_i \cdot \frac{\partial P_i}{\partial u} \right)\end{aligned}\quad ; \quad (\text{A.3})$$

and

$$\begin{aligned}\frac{\partial}{\partial \psi} \left(\vec{e}_i \cdot \frac{\partial P_i}{\partial u} \right) &= \frac{l_i}{r_i} \sin \theta_i \cos(\psi + \beta_i - \theta_i) = \\ &= \frac{\partial}{\partial u} \left(\vec{e}_i \cdot \frac{\partial P_i}{\partial \psi} \right) \\ \frac{\partial}{\partial \psi} \left(\vec{e}_i \cdot \frac{\partial P_i}{\partial v} \right) &= -\frac{l_i}{r_i} \cos \theta_i \cos(\psi + \beta_i - \theta_i) = \\ &= \frac{\partial}{\partial v} \left(\vec{e}_i \cdot \frac{\partial P_i}{\partial \psi} \right) \\ \frac{\partial}{\partial \psi} \left(\vec{e}_i \cdot \frac{\partial P_i}{\partial \psi} \right) &= -l_i \cos(\psi + \beta_i - \theta_i) \left(1 + \frac{l_i}{r_i} \cos(\psi + \beta_i - \theta_i) \right)\end{aligned}\quad (\text{A.4})$$

In fact, symmetries and recursive relations may be seen embedded in the expressions above.

B. Horizontal force function for a catenary line supported on a frictionless and horizontal seabed

Consider the i^{th} catenary line supported on a frictionless and horizontal seabed, as shown in Figure 15. L_i is the total length, from the anchor A_i to the fairlead P_i ; L_{si} is the suspended length; z_{fi} is the distance between the fairlead and the seabed; r_{si} and r_i are, respectively, the projections of the suspended and total length on the seabed. Let γ_i be the immersed weight per unit length and f_i the horizontal component of the tension at the fairlead.

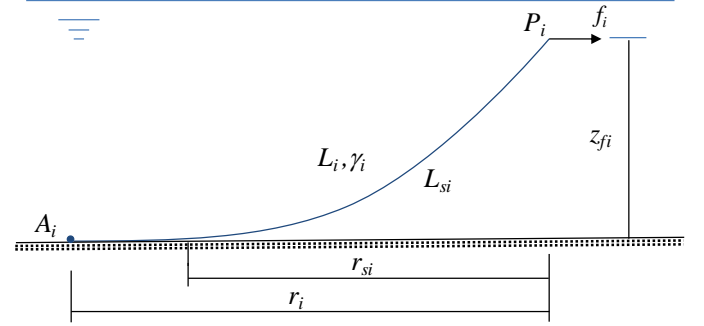


Figure 15: Catenary line and geometric definitions

From the classic equations of a catenary, by eliminating L_{si} and r_{si} in favor of L_i and r_i , it can be proved that, see e.g. [6], the function $f_i(r_i)$ may be written in an analytic, though inverse form, as

$$\begin{aligned}\frac{r_i(f_i)}{L_i} &= 1 - \frac{f_i}{\gamma_i L_i} \left[g(f_i) - \ln(h(i)) \right] \\ \text{with} \\ g(f_i) &= \left(\frac{1 + 2 f_i / \gamma_i z_{fi}}{(f_i / \gamma_i z_{fi})^2} \right)^{\frac{1}{2}}, \quad (\text{A.5})\end{aligned}$$

and

$$h(f_i) = 1 + \frac{\gamma_i z_{fi}}{f_i} + g(f_i)$$

from which the mooring line ‘derivative stiffness’ $k_i(r_i) = f_i'(r_i)$, as well as the ‘string stiffness’ $\bar{k}_i(r_i) = f_i(r_i)/r_i$ may be readily obtained.